



Catalytic degradation of tetracycline by Mo–Fe catalyst

Suli Zhi^a, Liang Tian^b, Nan Li^c, Keqiang Zhang^{a,*}

^aAgro-Environmental Protection Institute, Ministry of Agriculture, Tianjin 300191, China, Tel. +86 22 23616673; email: zhisuli87@163.com (S. Zhi), Tel. +86 22 23616689; email: keqiangzhang68@163.com (K. Zhang)

^bHebei University of Technology, Tianjin 300132, China, Tel. +86 15900390153; email: tianliangg@sina.com

^cWuhan Environmental Monitoring Center, Wuhan 430000, China, Tel. +86 13720301564; email: 13720301564@163.com

Received 6 November 2016; Accepted 12 May 2017

ABSTRACT

Incorporating Mo into Fe-catalyst can enhance the catalytic activity and application range of pH value of catalyst. Therefore, Mo–Fe compounds with different Mo:Fe molar ratios were prepared by a wet chemical process, and then were used to degrade tetracycline (TC) by initiating a heterogeneous Fenton-like system with H₂O₂. The results demonstrated that the Fe₂(MoO₄)₃/H₂O₂ system most efficiently degraded TC. At an initial concentration of 50 mg/L TC with natural pH value (about 5.5), about 99% of TC could be removed within 30 min by 0.8 g/L Fe₂(MoO₄)₃ and 17.6 mM H₂O₂ at 299.15 K. Moreover, the pH value did not affect TC removal rate; but changed the total organic carbon removal rate. The Fe leaching concentration was about 0.009 mg/L under the optimal conditions. The TC removal rates in the Fe₂(MoO₄)₃/H₂O₂ system were influenced by the complexity level of practical wastewater. The scavenging experiment using several scavengers indicated that both hydroxyl radicals (in solution and catalyst surface) and superoxide radicals played important roles in the degradation of TC. A possible degradation mechanism and pathway for TC were proposed in the Fe₂(MoO₄)₃/H₂O₂ system. Finally, a comparison was made between this study and some others, showing that Fe₂(MoO₄)₃/H₂O₂ was a preponderant system for TC removal.

Keywords: Mo–Fe catalyst; Hydrogen peroxide; Fenton-like; Tetracycline

1. Introduction

The presence of antibiotic residues in environmental matrices has attracted increasing attention due to the worldwide use of antibiotics in human therapy and the farming industry [1–3]. Especially, in China, approximately 162,000 tons of antibiotics were used in 2013, based on the survey by Zhang et al. [4]. Among of these antibiotics, tetracyclines (TCs) mainly including tetracycline (TC), oxytetracycline (OTC) and chlorotetracycline (CTC) are among the most important families of antibiotics that contaminate the environment. To date, TCs have been widely detected in different water sources, including rivers, streams, lakes and ground waters, many of which are used as drinking water sources [5–12]. The continuous releasing of TCs into

aquatic environments increases the possibility of antibiotic resistance among microbial populations, and the degradation by-products of TCs have been demonstrated to be even more toxic than the parent compounds [13,14]. In particular, TC is a typical one in TCs, which has been widely used, and many researchers have focused on the removal of TC [1–3]. Therefore, it is urgent to develop efficient and economical technologies to remove TCs (especially TC) from aquatic environments.

At present, there are many methods for removing TCs from water, including biodegradation [15,16], adsorption [14,17], ozonation [18], photodegradation [19,20], chemical oxidation [21–23], electrochemical oxidation [3,24,25] and so on. Of these methods, traditional biological methods cannot effectively destruct TCs due to their antibacterial nature and complex structure. Adsorption has further disadvantages because it only separates pollutants to another phase rather than mineralizing them [14,26]. Compared with chemical

* Corresponding author.

oxidation, ozonation, photodegradation and electrochemical oxidation might need additional equipment and more investment for practical application. Therefore, chemical oxidation is currently the preferred method for the removal of TCs.

Fenton or Fenton-like catalysis has emerged as an advanced oxidation technology to treat various non-biodegradable organic pollutants [27,28]. TCs removal was recently conducted by some researchers via advanced oxidation technology. Sunaric et al. [29] reported the effect of Cu(II)/H₂O₂ on doxycycline removal from aqueous solution, and Liu et al. [30] prepared Fe₃O₄-graphite cathode and it showed excellent electrocatalysis characteristic for TC degradation in electro-Fenton system. Hou et al. [31] used Fenton-based process (H₂O₂/Fe(III)) to remove TC, and 93.6% removal rate was obtained under optimal conditions. However, most of these Fenton-like catalysts had higher catalytic activity just at pH values around 3.0 resulting in the acidification of the wastewater or the input of external energy into reaction system [30,31], which generally increased the costs of wastewater treatment process.

The catalytic activity in a Fenton-like system mainly lies in the acid/base properties of the catalyst, which can be indicated by the PZC (pH at the point of zero charge). Lower PZC values correspond to a more acidic character [27], which results in stronger catalytic activity. Although the PZC values of α -Fe₂O₃, FeOOH and Fe₃O₄ are in a relatively low range, respectively, 5.2–8.6, 6.5–6.9 and 6.3–6.7 [32], the catalytic ability of these Fe-catalyst was limited under some conditions, especially under alkaline condition. Recently, incorporating other metal ions into Fe-catalyst could decrease the PZC and improve the acidic character, which could ensure stronger catalytic activity in a wide pH range [33]. Among these metals, Mo was an attractive one which could effectively decrease the PZC of catalyst. For example, the PZC values of 5 mol% Mo/TiO₂, 10 wt% MoO₃/Al₂O₃, 7.6 wt% MoO₃/ZrO₂, 0.5 wt% Mo/SiO₂ and Fe₂(MoO₄)₃ were found to be 2.2, 3.7, 2.5 and 2.9, respectively [27,34–37]. However, these reports did not involve antibiotics removal.

This study has synthesized the Mo–Fe catalyst with different ratios of Mo/Fe to degrade TC which was a typical one of TCs. The following aspects were investigated: (1) characteristics of catalyst powder; (2) catalytic activity of these different Mo–Fe catalysts in the presence of H₂O₂; (3) effect of operating factors of Fe₂(MoO₄)₃/H₂O₂ system on TC removal; (4) durability of Fe₂(MoO₄)₃ and Fe leaching; (5) degradation mechanism of TC in the Fenton-like system by Fe₂(MoO₄)₃/H₂O₂; (6) application of Fe₂(MoO₄)₃/H₂O₂ in real wastewater under optimal conditions and (7) comparison with other studies.

2. Materials and methods

2.1. Materials

Analytical grade ammonium molybdate(VI) tetrahydrate, iron(III) nitrate monohydrate, hydrogen peroxide solution (30%, w/v), ammonium hydroxide (25%, w/v), *n*-butanol, KI, benzoquinone, NaCl, HCl and NaOH were purchased from Tianjin Kermel Chemical Reagent Co. Ltd. (China). TC was purchased from J&K Scientific Ltd. (China).

The methyl alcohol, formic acid and acetonitrile were HPLC grade and purchased from Tianjin Kermel Chemical Reagent Co. Ltd. (China).

2.2. Preparation of catalysts

Fe₂(MoO₄)₃ was prepared by a previously reported wet chemical process [38,39]. Simply, a solution of 0.01 M ammonium molybdate was mixed with certain volume of 2 M ammonium hydroxide. Then a certain volume of 0.093 M iron nitrate was slowly added dropwise at room temperature into the mixed solution under vigorous agitation. After complete addition of iron nitrate, the solution was stirred for 2 h at room temperature. The resulting precipitate was filtered, and sequentially washed with deionized water and then dried at 105°C for 12 h. Finally, the dried precipitate was calcined in a muffle furnace at 550°C. The Fe–Mo catalyst with other Fe:Mo molar ratios was prepared in a similar way.

2.3. Experimental procedures

All experiments were carried out in plastic tubes with an effective volume of 10 mL. A given amount of catalyst powder was added in the reaction tube; then, 5 mL of the designed concentration of TC was added into the tubes. The concentrations of TC were set from 2 to 200 mg/L, which are the common concentrations according to the existing literatures [2,3,25]. The reaction was started by adding a known amount of hydrogen peroxide to the reaction tube. The reaction tubes were put into a concussion incubator working at 220 rpm. After the oxidation reaction, the samples were filtered with a 0.22 μm membrane to remove catalyst powder. Then, samples were diluted with deionized water and methyl alcohol.

2.4. Instruments and analytical methods

The morphologies of the catalyst powder at different Fe:Mo molar ratios were performed on gold-coated samples using field emission scanning electron microscope (FESEM, Nanosem 430). The element composition of each powder was determined by an energy dispersive spectrometer (EDS), which is accessory equipment with FESEM. The patterns of these catalyst powders were collected on powder X-ray diffraction (XRD, D/MAX-2500) using Cu-Kα radiation. Compound identification in the samples was accomplished by comparison of the peaks with joint committee on powder diffraction standards (JCPDS) data files. The pH at PZC was tested with a zeta potential analyzer (Zetasizer Nano ZS, Malvern). Fe leaching into solution during the reaction was detected by an atomic adsorption spectrometer (Beijing Ruili WFX 1300). The total organic carbon (TOC) at the optimized conditions was determined using a TOC analyzer (Shimadzu TOC-V).

Concentrations of TC were quantified by LC–MS/MS analysis, using Waters ACQUITY UPLC–AB SCIEX QTRAP®4500 with a ACQUITY UPLC®HSS T3 C18 COLUMN (2.1 mm × 100 mm, 1.8 μm). The injection volume was 2 μL, and the flow rate was 0.3 mL/min. The mobile phase A was methanol and B was 0.1% aqueous formic acid. The gradient elution was programmed as follows: phase A was 10% in 0–0.5 min, followed by ascending to 80% within 3.5 min, held for 2 min, then rose to 90% to 4.4 min, followed by a

ramp to 10% until to 5 min. The intermediates of TC were also determined by the LC–MS method with a time-of-flight mass spectrometer.

3. Results and discussion

3.1. Physicochemical properties of the catalyst

Different from previous study, different Mo/Fe ratios were set to study the effect of Mo content on the TC removal rate. Fig. 1 shows the XRD patterns of different catalyst powders with Mo and Fe at Mo:Fe = 0, 0.1, 0.2, 0.5, 0.9, 1.5. From the figure, it can be seen that powder with Mo/Fe = 0 had high XRD peaks at 2θ of 33.1° and 49.5° which are associated with α - Fe_2O_3 . With the increase of Mo/Fe ratio, the XRD patterns gradually showed more peaks. Powder with Mo/Fe = 0.5–1.5 all showed typical peaks at 19.4° , 20.4° , 21.7° , 22.9° , 23.6° , 24.9° , 25.7° , 27.5° , 27.8° , 30.2° and 34.1° , which are attributed to monoclinic $\text{Fe}_2(\text{MoO}_4)_3$. All these results were in accordance with a previous study [27].

Both SEM and EDS were performed to observe the element composition and morphology of the catalyst powder at different Mo/Fe ratios, shown in Figs. S1–S7. It can be seen that the Mo content increased with the increasing of Mo/Fe ratios, which indicated that incorporating into Mo worked effectively. However, the measured values of Mo/Fe were lower than the theoretical values, which may be due to that EDS was a semi-quantity method.

In order to determine the effect of incorporating into Mo on the PZC value of the Mo–Fe powder, two methods were adopted: (1) determining the pH value at zero zeta potential and (2) determining pH values by adding an increasing mass of these powders in 10 mL water. From Fig. S7(a), the PZC values for Fe_2O_3 and $\text{Fe}_2(\text{MoO}_4)_3$ were, respectively, 2.58 and 4.25 which implied that incorporating Mo into Fe-catalyst could decrease the PZC of catalyst powder. Seen from Fig. S7(b), with the increase of the powder dosage, the pH value tended to a constant point where PZC of these powders were obtained. For example, PZC of Fe_2O_3 and $\text{Fe}_2(\text{MoO}_4)_3$ was determined at about 5.08 and 2.69. The results were in accordance with the reported results [32]. It was explained that low surface deprotonation constant ($\text{p}K_a$ s) ensured low PZC

values [32,40]. $\text{p}K_a$, an indicator of acidic strength, decreases linearly as the ratio of charge to radius (z/r) increases [19,21]. Furthermore, Mo^{6+} has an ionic radius of 0.59 \AA at the coordination number of 6 [41]. It has very large z/r of 10.17 by calculation, which contributes to the low PZC value and consequently the high acidic strength of $\text{Fe}_2(\text{MoO}_4)_3$.

3.2. Catalytic activity of $\text{Fe}_2(\text{MoO}_4)_3$

In order to determine the catalytic ability of these catalyst powders at different Mo/Fe ratios, TC removal rates with catalyst powder were obtained under the same conditions, shown in Fig. 2. We can see that Mo/Fe molar ratios of 0.2 and 1.5 resulted in higher TC removal rates at about 99.64% and 99.65%, respectively. However, evaluating the XRD patterns of these powders, the powder with the Mo/Fe molar ratio of 1.5 had more anomalous crystal form. Therefore, $\text{Fe}_2(\text{MoO}_4)_3$ was optimal choice to create the heterogeneous Fenton-like system.

To ensure the catalytic ability of $\text{Fe}_2(\text{MoO}_4)_3$, the effects of H_2O_2 -only, $\text{Fe}_2(\text{MoO}_4)_3$ -only and $\text{Fe}_2(\text{MoO}_4)_3 + \text{H}_2\text{O}_2$ were compared in Fig. 3. It can be seen that the TC removal rates in

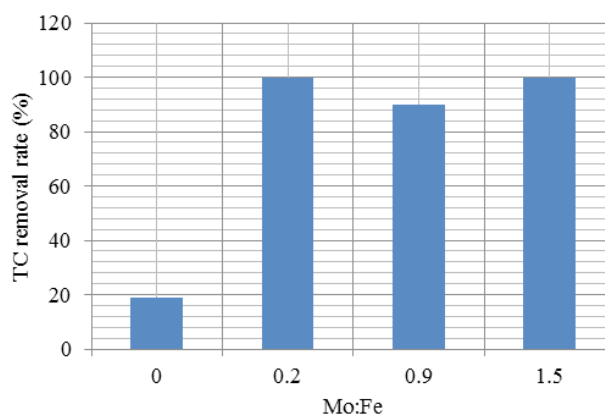


Fig. 2. Catalytic ability of catalyst powder at different Mo/Fe ratios (TC concentration 50 mg/L, catalyst dosage 2 g/L, H_2O_2 dosage 35 mM, natural solution pH, reaction time 60 min).

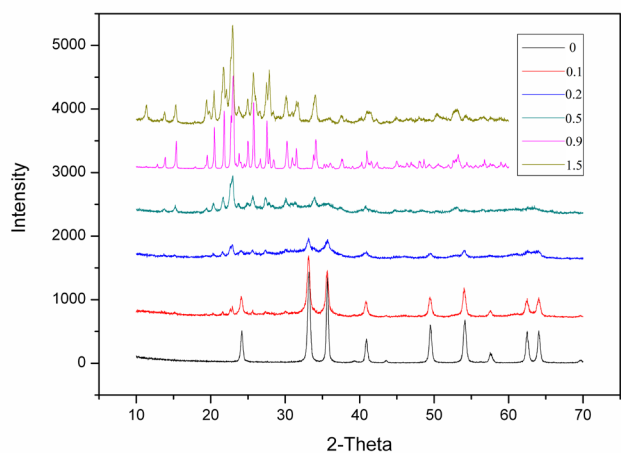


Fig. 1. XRD pattern of catalyst powder.

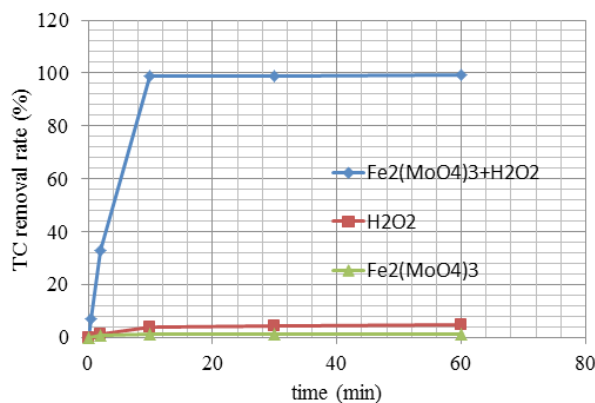


Fig. 3. Catalytic ability of $\text{Fe}_2(\text{MoO}_4)_3$ (TC concentration 50 mg/L, catalyst dosage 2 g/L, H_2O_2 dosage 35 mM, natural solution pH 5.5, reaction time 60 min).

the H_2O_2 -only system or the $\text{Fe}_2(\text{MoO}_4)_3$ -only system were so marginal that could be neglected. For example, the removal rates were about 4.69% and 1.02% in H_2O_2 -only system or $\text{Fe}_2(\text{MoO}_4)_3$ -only system after 60 min reaction. While in the system with both H_2O_2 and $\text{Fe}_2(\text{MoO}_4)_3$, more than 99% TC was removed after 60 min reaction, which indicated that $\text{Fe}_2(\text{MoO}_4)_3$ could act excellently as catalyst to oxidize TC. The Fenton-like reaction was created by the presence of H_2O_2 and $\text{Fe}_2(\text{MoO}_4)_3$.

3.3. Effect of operational conditions on TC removal

3.3.1. Effect of catalyst dosage and H_2O_2 concentration

Catalyst dosage is a primary factor not only in initiating the Fenton-like reaction by accelerating radical generation, but also in controlling the economic cost of the Fenton-like process by adjusting optimal dosage. Fig. 4 shows the experiment conducted with catalyst dosage in a range of 0–5 g/L while other parameters were kept constant. It can be seen that TC concentration in solution decreased sharply with the increasing of catalyst dosage. In a 60 min reaction, when the catalyst dosage increased from 0 mg/L to 0.8 g/L, the TC concentration in solution decreased from 50 to 0.28 mg/L (with a removal rate of 99.4%). Increasing dosage of $\text{Fe}_2(\text{MoO}_4)_3$ provided more $\text{Fe}^{2+}/\text{Fe}^{3+}$ active sites which accelerated radical generation and result in higher TC removal rate. However, another report showed that increasing $\text{Fe}_2(\text{MoO}_4)_3$ dosage from 0.8 to 1.6 g/L just resulted in AOII removal rate increasing from about 80% to 97% [27]. Obviously, the $\text{Fe}_2(\text{MoO}_4)_3$ dosage in this study was lower and removal rate was higher, which means $\text{Fe}_2(\text{MoO}_4)_3$ could effectively start the Fenton-like reaction at very low dosage for TC removing.

In addition, Fig. 4 shows that higher concentrations of H_2O_2 resulted in higher TC removal rates. When the concentration of H_2O_2 was increased from 7.0 to 17.6 mmol/L, the removal rate of TC also increased from 84.4% to 98.8%. However, a concentration of 88.2 mmol/L H_2O_2 just increased TC removal rate to 99.6%. It may be due to that higher H_2O_2

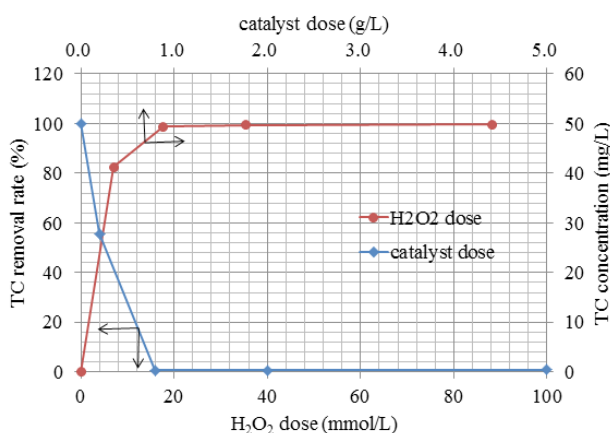


Fig. 4. TC removal at different catalyst dosage and H_2O_2 concentration (TC concentration 50 mg/L, catalyst dosage 2 g/L or H_2O_2 dosage 35 mM, natural solution pH 5.5, reaction time 60 min).

concentrations might result in the scavenging reaction of $\cdot\text{OH}$ by H_2O_2 as follows [31,42]:



OH is consumed by H_2O_2 to produce $\text{HO}_2\cdot$ which is much less reactive than $\cdot\text{OH}$ and can hardly contribute to the oxidation of TC.

Therefore, the optimal catalyst dosage and H_2O_2 concentration were 0.8 g/L of $\text{Fe}_2(\text{MoO}_4)_3$ and 17.6 mM of H_2O_2 .

3.3.2. Effect of reaction time and initial TC concentration

In order to determine the effect of the Fenton-like system, we conducted the experiments with different reaction times and different initial concentrations, as shown in Fig. 5, TC removal rates rose rapidly with reaction time at the initial stage. Under different initial TC concentrations, TC removal rates all reached >90% with the reaction time of 10 min. Hence, a reaction time of 30 min was sufficient to ensure all the removal rates in a range of 97%–98%, under different initial TC concentrations. Moreover, initial TC concentration varied from 20 to 200 mg/L seemed to have no influence on the TC removal rates, which demonstrated the excellent catalytic effect of $\text{Fe}_2(\text{MoO}_4)_3$ on TC removal.

3.3.3. Effect of initial solution pH

The pH value is usually considered as one of the most important factors during Fenton-like processes; it controls the decomposition pathways of H_2O_2 and catalyst activity. In addition, the speciation of TC also depends on pH value by the protonation–deprotonation equilibrium as shown in Fig. 6. It is known that at low pH values (<3.3), TC was fully protonated as H_3L^+ ; at slightly higher pH (>3.3), TC was mainly in the form of H_2L^+ by releasing enolic proton at C-3; at further higher pH (>7.7), HL^- was formed by the dissociation of the hydroxyl proton attaching to C-12.

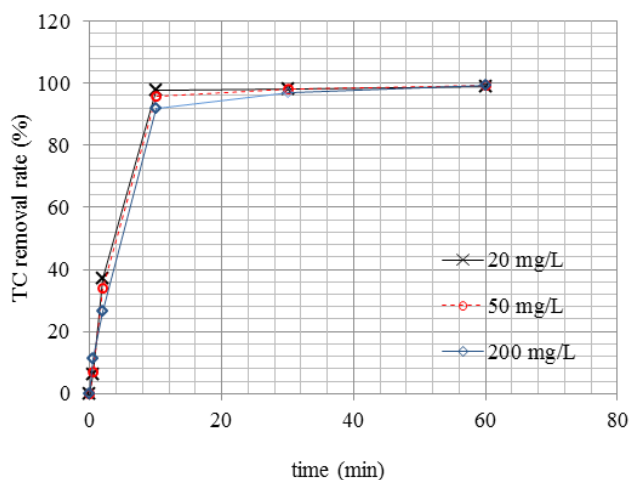


Fig. 5. TC removal at different reaction time and initial TC concentration (catalyst dosage 2 g/L, H_2O_2 dosage 35 mM, natural solution pH 5.5).

Generally, when HL^- formed at $pH > 7.7$, the catalyst surface would become negatively charged causing repulsion with negatively charged TC molecules, which was the reason for the decrease of TC removal rate in many studies [23,31,44,50,51]. However, in our study, $Fe_2(MoO_4)_3$ seemed to be unaffected by the initial pH values, as shown in Fig. 7. TC removal rates were relatively stable with the pH values from 3.0 to 10.0, indicating that $Fe_2(MoO_4)_3$ could maintain high catalytic activity in a wide range of pH value. Up to now, many reports have shown that the performance of catalysts in oxidation processes would become poor with the increasing of initial pH value. In a report where TC was treated with Fe–Mn binary oxide, the removal rate was found to be maximum in the pH range 5.3–6.2 [43]. In another report, Mahamallik et al. [44] pointed out that acetic acid–sodium acetate buffer solution could be used to maintain pH in the acidic range 3.4–6.1 for a higher TC removal rate. In this study, initial pH values did not seem to affect TC removal rates, which means

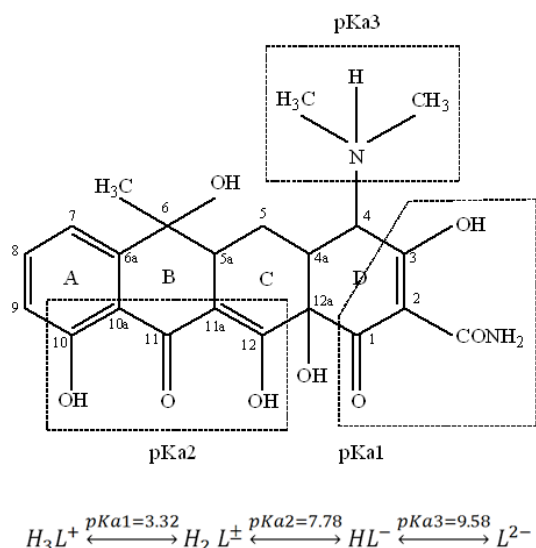


Fig. 6. Different ionic forms of TC molecule with respect to pK_a values.

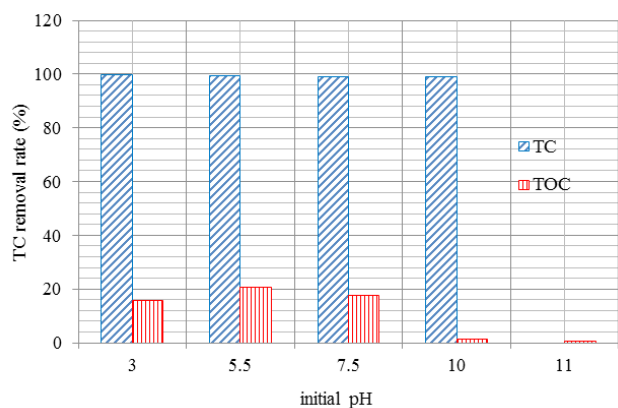


Fig. 7. TC removal at different pH value (TC concentration 50 mg/L, catalyst dosage 2 g/L, H_2O_2 dosage 35 mM, reaction time 60 min).

the wide pH application scope of $Fe_2(MoO_4)_3$. However, the disappearance of TC did not mean the complete mineralization of TC to CO_2 .

To evaluate the effect of the initial pH values on TC mineralization, TOC was investigated at different pH values. From Fig. 7, TOC removal rates changed with the solution pH. The highest TOC removal rate was obtained at pH of 5.5, where no HCl or NaOH was added to adjust solution pH. The TOC removal rates were somewhat lower at pH of 3.0 and 7.5, which primarily because the adjusting pH value made some inorganic ion adsorbed to the surface of $Fe_2(MoO_4)_3$ particles. Moreover, the lowest TOC removal rate was obtained at pH of 10.0. The reason was that the alkaline environment made the catalyst surface coated with large numbers of OH^- . Both tetracycline species and the catalyst carried more negative charge under the alkaline condition, leading to an enhancement in electrostatic repulsion between TC molecules and the catalyst particles. This may account for the decrease of the TOC removal.

3.3.4. Effect of ion strength (NaCl)

In oxidation processes, different ionic strength may affect the removal of the target organisms. Therefore, the experiment with different NaCl concentrations was conducted to study the effect of ion strength on TC removal rates. From Fig. 8, TC removal rates slightly decreased with the increase of NaCl concentration. When NaCl concentrations were 0, 0.01, 0.05 and 0.1 mol/L, the TC removal rates were 94.99%, 93.02%, 91.88% and 87.71%, respectively. Overall, the presence of NaCl had little influence on TC removal rate in the Fenton-like system with $Fe_2(MoO_4)_3$ and H_2O_2 .

3.4. Durability of $Fe_2(MoO_4)_3$ and Fe leaching

To investigate the stability of $Fe_2(MoO_4)_3$, TC removal rate of the recycled $Fe_2(MoO_4)_3$ was investigated under the optimum conditions. After each degradation experiment, the used catalyst powder was regenerated by drying in an oven at $100^\circ C$ for 4 h. Then the catalyst was reused under the same condition to remove TC. The results demonstrated that the catalyst activity just had a slight decrease during the three

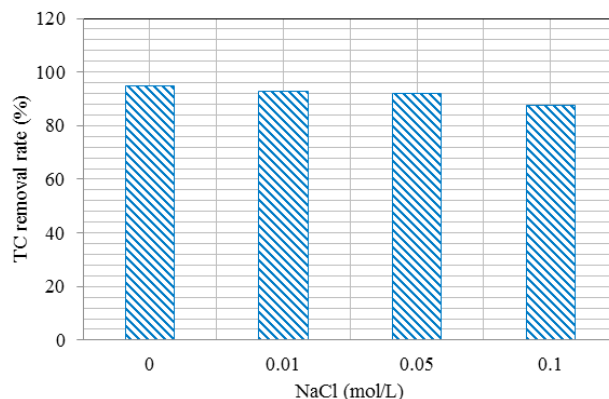


Fig. 8. TC removal at different NaCl content (TC concentration 50 mg/L, catalyst dosage 2 g/L, H_2O_2 dosage 35 mM, reaction time 60 min).

successive cycles (Fig. S8). This showed that $\text{Fe}_2(\text{MoO}_4)_3$ had strong stability.

Metals in heterogeneous catalysts tend to leach out during the reaction, which could affect the durability of catalyst resulting in influence on removal rate and reaction pathways [45]. Concentrations of Fe in the solution under different conditions were detected, as shown in Fig. 9. We can see that Fe concentration was highest at pH = 3.0 than those at other pH values. At under the natural solution pH of 5.5, the Fe concentration had a little increase (0–0.026 mg/L) with reaction time (0–60 min) under different initial TC concentrations. However, when the H_2O_2 dosage was doubled, the leaching concentration of Fe sharply rose to 1.28 mg/L at 120 min. Clearly, the reason for this is that more H_2O_2 attacked the catalyst resulting in a high Fe concentration. As a result, under the optimal conditions of catalyst dosage 0.08 g/L, H_2O_2 dosage 17.6 mM, natural pH value, reaction time 30 min and initial TC 50 mg/L, the Fe leaching concentration was approximately 0.009 mg/L.

3.5. Degradation mechanism

3.5.1. TOC removal

TOC removal was evaluated to determine the extent of TC oxidation. Then, the TOC removal rates were investigated under different initial TC concentrations, which were compared with TC removal rates under the same conditions (Fig. 10). TOC removal mainly occurred during the initial 10 min of the reaction and after 10 min no obvious TOC removal took place. This may be due to the pH change made the catalyst unsuitable for further TC degradation [44]. The most interesting finding was that TOC removal rates did not change with the initial TC concentrations. The reason may be that the degradation products of TC were definite, regardless of different initial TC concentrations. Furthermore, TOC removal rates were compared with TC removal rates in Fig. 10, showing that TC could easily be degraded under different initial concentrations, but it was not thoroughly degraded to CO_2 . The specific degradation intermediates analysis will be shown in section 3.5.4.

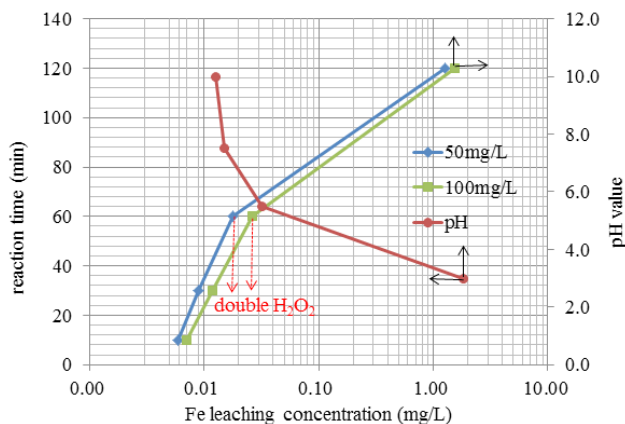


Fig. 9. Fe leaching at different conditions (catalyst dosage 0.08 g/L, H_2O_2 dosage 17.6 mM).

3.5.2. Effect of the presence of radical scavengers

In a Fenton-like system, there may be two kinds of radicals that have strong oxidation ability to degrade organic pollutants: $\cdot\text{OH}$ and $\text{O}_2^{\cdot-}$. In order to understand the oxidation mechanism, *n*-butyl alcohol (*n*-BuOH), KI and benzoquinone (BQ) usually were used to verify the roles of the total hydroxyl radicals both in the solution and on the surface of the catalyst ($\cdot\text{OH}_{\text{total}}$), the hydroxyl radicals in solution ($\cdot\text{OH}_{\text{free}}$) and $\text{O}_2^{\cdot-}$ radicals, respectively [23,31,45]. Experiment 1 was conducted with 350 mM *n*-BuOH, 7 mM KI and 2.5 mM BQ according to the report by Li et al. [45]. However, according to Fig. 11, no obvious decrease of TC removal rate was observed compared to the run with no radical scavengers. This may be due to the excess production of radicals to reduce TC and the radical scavengers may have just quenched a fraction of total radicals.

Experiment 2 was conducted by adding excess of radical scavengers with 1.0 M *n*-BuOH, 0.02 M KI and 0.02 M BQ. It can be seen that TC removal rates were decreased to 21%, 45% and 82% after adding *n*-BuOH, KI and BQ, respectively. These results revealed the important role of hydroxyl radicals in the Fenton-like system and that the oxidizing process

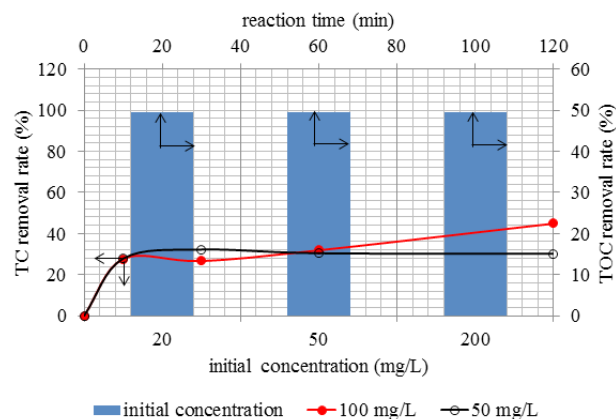


Fig. 10. TOC removal rate at different initial TC concentration (catalyst dosage 0.08 g/L, H_2O_2 dosage 17.6 mM, natural pH value).

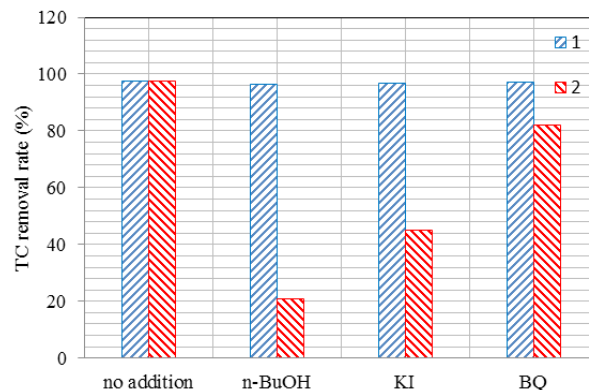
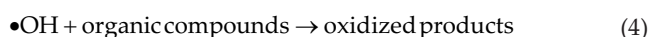
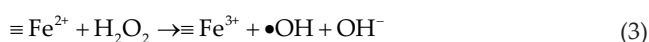


Fig. 11. TOC removal rate at different radical scavengers (catalyst dosage 0.08 g/L, H_2O_2 dosage 17.6 mM, natural pH value, reaction time 60 min, *n*-BuOH 350 and 1000 mM, KI concentration 7.0 and 20 mM, BQ 2.5 and 20 mM).

is more relevant to the hydroxyl radicals produced from the surface of $\text{Fe}_2(\text{MoO}_4)_3$ than that of in the bulk solution. Moreover, TC degradation efficiency was inhibited in the presence of BQ which indicated that O_2^- was also an important reactive oxygen species during the Fenton-like process. Based on the above analysis, TC degradation occurred by the combined effects of $\cdot\text{OH}$ in the solution and at the surface of the catalyst and O_2^- .

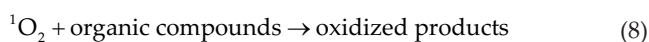
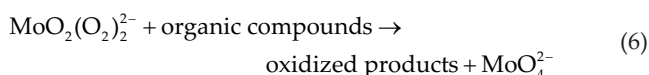
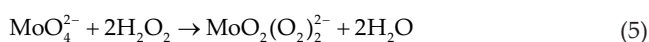
3.5.3. Catalytic mechanism of $\text{Fe}_2(\text{MoO}_4)_3$

It is well known that the Fenton-like system of $\text{Fe}/\text{H}_2\text{O}_2$ involves the reduction of Fe^{3+} to Fe^{2+} (Eq. (2)). Then, Fe^{2+} reacts with H_2O_2 to generate $\cdot\text{OH}$ radicals (Eq. (3)), which is a kind of very active radicals and can degrade the organic compounds (Eq. (4)) [46].



From the result of section 3.5.2, $\cdot\text{OH}$ was the main radical to oxidize TC, which clarify the presence of Eq. (2)–(4).

In addition, the $\text{MoO}_4^{2-}/\text{H}_2\text{O}_2$ system has been reported to oxidize different organic compounds [27,47]. The mechanism involves the formation of $\text{MoO}_2(\text{O}_2)_2^{2-}$ (Eq. (5)), which is a kind of strong oxidant that can oxidize the organic compounds by the direct oxygen transfer (Eq. (6)) [48] or by the singlet oxygen ($^1\text{O}_2$) generated from the peroxy complex (Eqs. (7) and (8)) [27,49].



Based on the above results, the oxidation mechanism for degradation of TC by the $\text{Fe}_2(\text{MoO}_4)_3/\text{H}_2\text{O}_2$ system was proposed, as shown in Fig. 12. In the traditional Fe Fenton system, H_2O_2 reacted with $\text{Fe}^{2+}/\text{Fe}^{3+}$ to produce $\cdot\text{OH}/\text{O}_2^-$ which were the main species to mineralize TC in the solution. However, in the Fe–Mo Fenton-like system, introducing into Mo leads to two results: (1) Mo enhanced the surface acidity of catalyst (blue area in Fig. 12), which accelerates the existing mechanism in the Fe Fenton system resulting in more $\cdot\text{OH}/\text{O}_2^-$ in the Fe–Mo catalyst surface or reaction solution and (2) $\text{MoO}_2(\text{O}_2)_2^{2-}$ produces in the Fe–Mo catalyst surface or reaction solution, which is an active species to oxidize TC (Eq. (6)). In addition, a kind of very active species of $^1\text{O}_2$ is

produced with $\text{MoO}_2(\text{O}_2)_2^{2-}$ translating into MoO_4^{2-} (Eq. (7)). Above all, introducing Mo into catalyst not only improved the existing oxidation reaction, but also produced additional two kinds of active species. All this would result in higher TC removal rate.

3.5.4. Degradation intermediates analysis under the optimal operation conditions

To determine the degradation products of TC in the Fenton-like system, LC–ESI–MS analysis was employed. The samples were obtained at different reaction times to clarify the oxidative degradation pathway of TC. Intermediates with m/z values of 476, 406, 185 and 113 were formed during the Fenton-like system at different reaction time. According to the results, a plausible degradation pathway is proposed in Fig. 13. The parent TC molecules were quickly oxidized

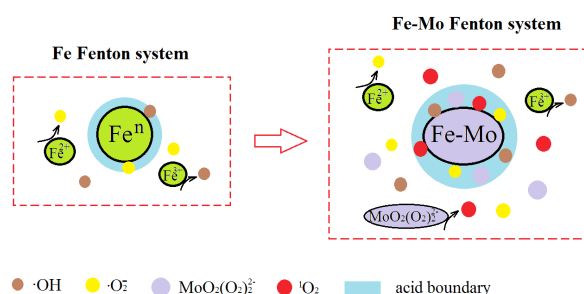


Fig. 12. Proposed mechanism of $\text{Fe}_2(\text{MoO}_4)_3/\text{H}_2\text{O}_2$ system.

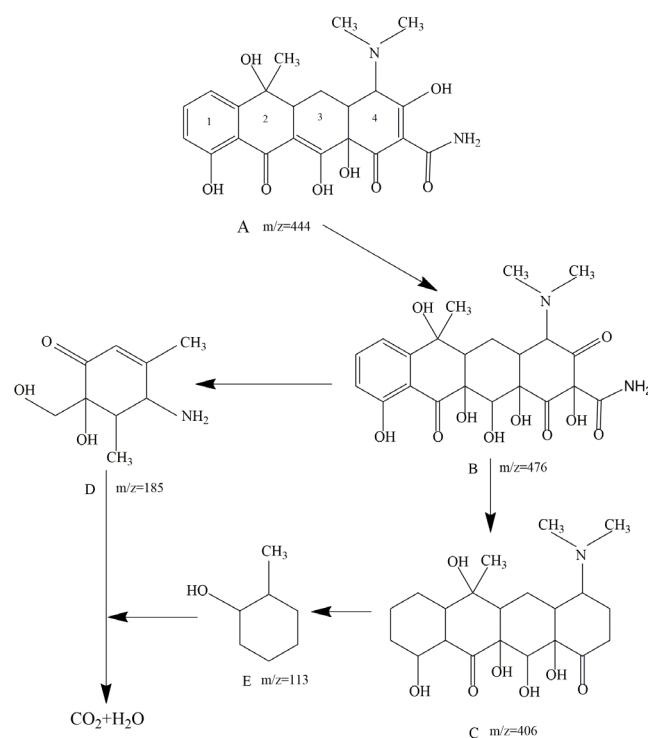


Fig. 13. Degradation intermediates of TC (catalyst dosage 0.08 g/L, H_2O_2 dosage 17.6 mM, natural pH value, reaction time 60 min).

and transformed into molecule B with m/z of 476 by open double bonds in rings 4 and 5. Subsequently, intermediate B lost the side chains of $O=C-NH_2$ and the double bonds in ring 1 was opened, forming product C with $m/z = 406$. Smaller molecules might be produced with the reaction, like intermediates D and E. As reported by Dalmázio et al. [50], products B and C formed in TC solution oxidized by ozone. Moreover, products D and E were obtained by Fu et al. [21] in a nanoscale zero-valent iron system to oxidize TC. Many other products with m/z of 417, 415, 372, 304, 174, 134, 197 and 160 were proposed in other reports [21], but they were not clearly determined in this study. The reason was that the degradation pathway was complex and might be influenced by many factors, including the catalyst, operating conditions and impurities in solution.

3.6. Application in real wastewater

From the above analysis, we see that $Fe_2(MoO_4)_3 + H_2O_2$ had excellent performance for TC removal in a pure water solution. For oxidation process of TC, most studies focused on the pure water solution of TC. However, the effect of

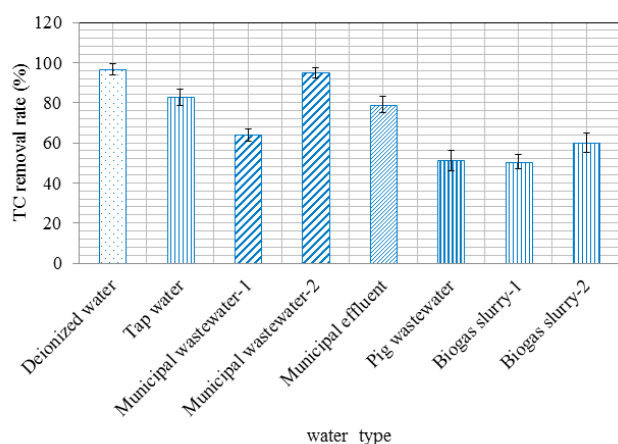


Fig. 14. Degradation of TC in real wastewater (catalyst dosage 0.08 g/L, H_2O_2 dosage 17.6 mM, natural pH value, reaction time 60 min).

Table 1

Comparison of TC degradation in this study with other studies under optimal conditions

System type	Initial TC concentration (mg/L)	Catalyst (g/L)	Oxidizing agent (mM)	Ultrasonic intensity (W)	Reaction time (min)	Solution pH value	TC removal rate (%)	References
US/ Fe_3O_4/H_2O_2	100	1.0	150	80	60	3.7	93.6	[31]
US/ $Fe_3O_4/Na_2S_2O_8$	100	1.0	400 ^a	80	90	3.7	89.0	[23]
MnO_2	50	1.0	–	–	20	4.0	55%	[44]
Fe^{2+}/H_2O_2	40	5	71.5	–	75	2.7 ± 0.1	60	[51]
Photo/ Fe^{2+}/H_2O_2	40	5	71.5	–	45	2.7 ± 0.1	77	
$Fe_3O_4@C/H_2O_2$	43.7	0.11	1.97	–	44	3.0 ± 0.2	79.25	[52]
$Fe_2(MoO_4)_3/H_2O_2$	50	0.8	17.65	–	10	no pH limiting	>99	This study

^aOxidizing agent was $Na_2S_2O_8$.

the oxidation process of TC will be weakened in practical wastewater application. To date, few studies investigate the oxidation of TC in practical wastewater applications. Fig. 14 shows the effects of Fenton-like system by the $Fe_2(MoO_4)_3$ and H_2O_2 on TC removal in different wastewater solutions. Regarding deionized water solution as reference, tap water resulted in 13.82% decrease of TC removal (from 96.52% to 82.68%) under the same conditions. When municipal wastewater was used (municipal wastewater-1 in Fig. 14), just a 63.87% removal rate of TC was obtained under the same condition, compared with 96.52% in the deionized water solution. However, when the catalyst and H_2O_2 dosages were doubled for municipal wastewater (municipal wastewater-2 in Fig. 14), TC removal rate was increased to 94.85% which was approximately the same level as the deionized water solution. Therefore, to obtain the same removal rate of TC with deionized water, the dosage must be doubled to eliminate the effects of matrix. For municipal effluent, the obtained optimal catalyst and H_2O_2 dosage resulted in a 79.05% removal rate of TC, which was higher than that of municipal influent wastewater-1 (63.87%) under the same conditions. Hence, the more complicated of wastewater was, the lower the removal rate of TC, under same conditions. In addition, pig wastewater and biogas slurry water were obtained from a pig farm in Tianjin, to study the effect of this Fenton-like system for TC removal in more complex wastewater. From Fig. 14, we can see that pig wastewater and biogas slurry (biogas slurry-1) resulted in removal rates of 51.14% and 50.47%, respectively. When the catalyst and H_2O_2 dosages were doubled for the biogas slurry (biogas slurry-2 in Fig. 14), the TC removal rate was increased to 60.02%, just a 9.55% increase of TC removal rate at the expense of the double dosage of the catalyst and H_2O_2 . From the above analysis, it can be concluded that the more complex wastewater composition resulted in a lower TC removal rate, and increasing the catalyst and H_2O_2 dosage may solve the problem to a certain degree which inevitably caused the cost increasing.

3.7. Comparison with other studies

The operating parameters and TC removal rates were compared with some other relevant reports, which are summarized in Table 1.

(1) The TC removal rate in this study was close to >99% which was superior to that in other reports; (2) it only took 10 min to reach to the maximum TC removal rate, while it usually takes much more time in the comparison research; (3) the most important was that the Fenton-like system could remove TC in a large range of pH values. However, the pH values in most of compared studies were limited to the acidic range (usually around 3.0), which would increase investment for adjusting pH value in practical application; (4) regarding the catalyst and H₂O₂ usage, it was less than that in most other reports, except for Fe₃O₄@C/H₂O₂ system in reference [52]; (5) no excess energy in the forms of ultrasound, ultraviolet radiation or others was input in this study compared to those in references [23] and [31].

Considering all conditions and results, the Fe₂(MoO₄)₃/H₂O₂ system is a beneficial method for industrial application.

4. Conclusions

Mo–Fe catalyst with H₂O₂ was first used to degrade TC under different operating factors. The results showed that Fe₂(MoO₄)₃ could effectively initiate a heterogeneous Fenton-like system to degrade TC. Initial TC concentrations and pH values seemed to have no effect on TC removal rates, but they affected TOC removal rates. Both hydroxyl radicals and superoxide anions were the reactive species responsible for TC degradation after conducting the scavenging experiment, based on which a degradation mechanism was proposed. LC–MS was used to determine the intermediates of TC in the Fe₂(MoO₄)₃/H₂O₂ system. The effect of Fe₂(MoO₄)₃/H₂O₂ system on TC removal was investigated in several practical wastewater, and this system was compared with some other studies in detail.

Acknowledgment

This research was funded by China Postdoctoral Science Foundation (2016M601193) and Nation Science Foundation Project of China (41371481).

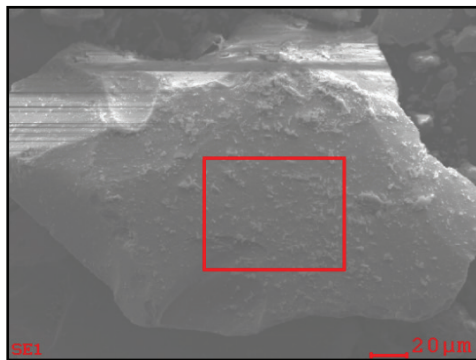
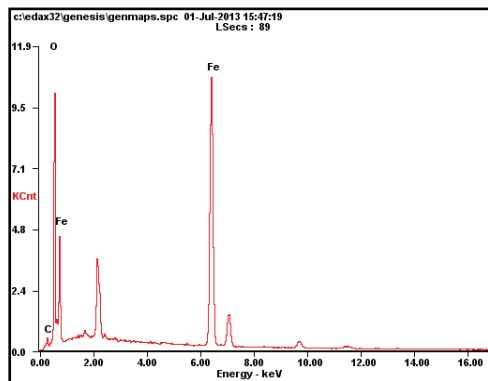
References

- [1] G. Hou, X. Hao, R. Zhang, J. Wang, R. Liu, C. Liu, Tetracycline removal and effect on the formation and degradation of extracellular polymeric substances and volatile fatty acids in the process of hydrogen fermentation, *Bioresour. Technol.*, 212 (2016) 20–25.
- [2] J.M. Lv, Y.L. Ma, X. Chang, S.B. Fan, Removal and removing mechanism of tetracycline residue from aqueous solution by using Cu-13X, *Chem. Eng. J.*, 273 (2015) 247–253.
- [3] J. Wu, H. Zhang, N. Oturan, Y. Wang, L. Chen, M.A. Oturan, Application of response surface methodology to the removal of the antibiotic tetracycline by electrochemical process using carbon-felt cathode and DSA (Ti/RuO₂–IrO₂) anode, *Chemosphere*, 87 (2012) 614–620.
- [4] Q.Q. Zhang, G.G. Ying, C.G. Pan, Y.S. Liu, J.L. Zhao, Comprehensive evaluation of antibiotics emission and fate in the river basins of China: source analysis, multimedia modeling, and linkage to bacterial resistance, *Environ. Sci. Technol.*, 49(2015) 6772–6782.
- [5] Y. Luo, L. Xu, M. Rysz, Y. Wang, H. Zhang, P.J.J. Alvarez, Occurrence and transport of tetracycline, sulfonamide, quinolone, and macrolide antibiotics in the Haihe River Basin, China, *Environ. Sci. Technol.*, 45 (2011) 1827–1833.
- [6] X. Yang, R.C. Flowers, H.S. Weinberg, P.C. Singer, Occurrence and removal of pharmaceuticals and personal care products (PPCPs) in an advanced wastewater reclamation plant, *Water Res.*, 45 (2011) 5218–5228.
- [7] A.L. Batt, S. Kim, D.S. Aga, Comparison of the occurrence of antibiotics in four full-scale wastewater treatment plants with varying designs and operations, *Chemosphere*, 68 (2007) 428–435.
- [8] P. Gao, M. Munir, I. Xagorarakis, Correlation of tetracycline and sulfonamide antibiotics with corresponding resistance genes and resistant bacteria in a conventional municipal wastewater treatment plant, *Sci. Total Environ.*, 421–422 (2012) 173–183.
- [9] R. Wei, F. Ge, S. Huang, M. Chen, R. Wang, Occurrence of veterinary antibiotics in animal wastewater and surface water around farms in Jiangsu Province, China, *Chemosphere*, 82 (2011) 1408–1414.
- [10] A.L. Spongberg, J.D. Witter, J. Acuña, J. Vargas, M. Murillo, G. Umaña, E. Gómezb, G. Perezc, Reconnaissance of selected PPCP compounds in Costa Rican surface waters, *Water Res.*, 45 (2011) 6709–6717.
- [11] Y. Bai, W. Meng, J. Xu, Y. Zhang, C. Guo, Occurrence, distribution and bioaccumulation of antibiotics in the Liao River Basin in China, *Environ. Sci. Processes Impacts*, 16 (2014) 586–593.
- [12] D. Cheng, X. Liu, L. Wang, W. Gong, G. Liu, W. Fu, M. Cheng, Seasonal variation and sediment-water exchange of antibiotics in a shallower large lake in North China, *Sci. Total Environ.*, 476–477 (2014) 266–275.
- [13] J. Jeong, W. Song, W.J. Cooper, J. Jung, J. Greaves, Degradation of tetracycline antibiotics: mechanisms and kinetic studies for advanced oxidation/reduction processes, *Chemosphere*, 78 (2010) 533–540.
- [14] M. Liu, L. Hou, S. Yu, B. Xi, Y. Zhao, X. Xia, MCM-41 impregnated with A zeolite precursor: synthesis, characterization and tetracycline antibiotics removal from aqueous solution, *Chem. Eng. J.*, 223 (2013) 678–687.
- [15] B. Li, T. Zhang, Biodegradation adsorption of antibiotics in the activated sludge process, *Environ. Sci. Technol.*, 44 (2010) 3468–3473.
- [16] L. Huang, X. Wen, Y. Wang, Y. Zou, B. Ma, X. Liao, J. Liang, Y. Wu, Effect of the chlortetracycline addition method on methane production from the anaerobic digestion of swine wastewater, *J. Environ. Sci.*, 26 (2014) 2001–2006.
- [17] Y. Lin, S. Xu, L. Jia, Fast and highly efficient tetracyclines removal from environmental waters by graphene oxide functionalized magnetic particles, *Chem. Eng. J.*, 225 (2013) 679–685.
- [18] Z.R. Hopkins, L. Blaney, A novel approach to modeling the reaction kinetics of tetracycline antibiotics with aqueous ozone, *Sci. Total Environ.*, 468–469 (2014) 337–344.
- [19] C. Zhao, Y. Zhou, D.J. Ridder, J. Zhai, Y. Wei, H. Deng, Advantages of TiO₂/5A composite catalyst for photocatalytic degradation of antibiotic oxytetracycline in aqueous solution: Comparison between TiO₂ and TiO₂/5A composite system, *Chem. Eng. J.*, 248 (2014) 280–289.
- [20] C.C. Yang, C.L. Huang, T.C. Cheng, H.T. Lai, Inhibitory effect of salinity on the photocatalytic degradation of three sulfonamide antibiotics, *Int. Biodeterior. Biodegrad.*, 102 (2015) 116–125.
- [21] Y. Fu, L. Peng, Q. Zeng, Y. Yang, H. Song, J. Shao, S. Liu, J. Gu, High efficient removal of tetracycline from solution by degradation and flocculation with nanoscale zerovalent iron, *Chem. Eng. J.*, 270 (2015) 631–640.
- [22] P. Wang, Y.L. He, C.H. Huang, Reactions of tetracycline antibiotics with chlorine dioxide and free chlorine, *Water Res.*, 45 (2011) 1838–1846.
- [23] L. Hou, H. Zhang, X. Xue, Ultrasound enhanced heterogeneous activation of peroxydisulfate by magnetite catalyst for the degradation of tetracycline in water, *Sep. Purif. Technol.*, 84 (2012) 147–152.
- [24] L. Xu, Y. Sun, L. Du, J. Zhang, Removal of tetracycline hydrochloride from wastewater by nanofiltration enhanced by electro-catalytic oxidation, *Desalination*, 352 (2014) 58–65.

- [25] Y.A. Ouaisa, M. Chabani, A. Amrane, A. Bensmaili, Removal of tetracycline by electrocoagulation: kinetic and isotherm modeling through adsorption, *J. Environ. Chem. Eng.*, 2 (2014) 177–184.
- [26] J. Ma, M. Yang, F. Yu, J. Chen, Easy solid-phase synthesis of pH-insensitive heterogeneous CNTs/FeS Fenton-like catalyst for the removal of antibiotics from aqueous solution, *J. Colloid Interface Sci.*, 444 (2015) 24–32.
- [27] S.H. Tian, Y.T. Tu, D.S. Chen, X. Chen, Y. Xiong, Degradation of Acid Orange II at neutral pH using $\text{Fe}_2(\text{MoO}_4)_3$ as a heterogeneous Fenton-like catalyst, *Chem. Eng. J.*, 169 (2011) 31–37.
- [28] E.G. Garrido-Ramirez, B.K.G. Theng, M.L. Mora, Clays and oxide minerals as catalysts and nanocatalysts in Fenton-like reactions—a review, *Appl. Clay Sci.*, 47 (2010) 182–192.
- [29] S.M. Sunaric, S.S. Mitic, G.Z. Miletic, A.N. Pavlovic, D. Naskovic-Djokic, Determination of doxycycline in pharmaceuticals based on its degradation by $\text{Cu(II)/H}_2\text{O}_2$ reagent in aqueous solution, *J. Anal. Chem.*, 64 (2009) 231–237.
- [30] S. Liu, X. Zhao, H. Sun, R. Li, Y. Fang, Y. Huang, The degradation of tetracycline in a photo-electro-Fenton system, *Chem. Eng. J.*, 231 (2013) 441–448.
- [31] L. Hou, L. Wang, S. Royer, H. Zhang, Ultrasound-assisted heterogeneous Fenton-like degradation of tetracycline over a magnetite catalyst, *J. Hazard. Mater.*, 302 (2016) 458–467.
- [32] G.A. Parks, The isoelectric points of solid oxides, solid hydroxides, and aqueous hydroxo complex systems, *Chem. Rev.*, 65 (1965) 177–198.
- [33] J.H. Deng, J.Y. Jiang, Y.Y. Zhang, X.P. Lin, C.M. Du, Y. Xiong, Ya, FeVO_4 as a highly active heterogeneous Fenton-like catalyst towards the degradation of Orange II, *Appl. Catal., B*, 84 (2008) 468–473.
- [34] Y. Anjaneyulu, N.S. Chary, D.S.S. Raj, Decolourization of industrial effluents available methods and emerging technologies—a review, *Rev. Environ. Sci. Biotechnol.*, 4 (2005) 245–273.
- [35] E. Hillerova, M. Zdrzil, Effect of loading on hydrodesulfurization activity of $\text{Mo/Al}_2\text{O}_3$ and Mo/C sulfide catalysts prepared by slurry impregnation with molybdic acid, *Appl. Catal., A*, 138 (1996) 13–26.
- [36] L. Kaluza, M. Zdrzil, Slurry impregnation of ZrO_2 extrudates: controlled eggshell distribution of MoO_3 , hydrodesulfurization activity, promotion by Co, *Catal. Lett.*, 127 (2009) 368–376.
- [37] S.D. Kohler, J.G. Ekerdt, D.S. Kim, I.E. Wachs, Relationship between structure and point of zero surface charge for molybdenum and tungsten oxides supported on alumina, *Catal. Lett.*, 16 (1992) 231–239.
- [38] C. Peng, L. Gao, S.W. Yang, J. Sun, A general precipitation strategy for large-scale synthesis of molybdate nanostructures, *Chem. Commun.*, 43 (2008) 5601–5603.
- [39] W.M. Shaheen, Thermal behaviour of pure and binary $\text{Fe}(\text{NO}_3)_3 \cdot 9\text{H}_2\text{O}$ and $(\text{NH}_4)_6\text{Mo}_7\text{O}_{24} \cdot 4\text{H}_2\text{O}$ systems, *Mater. Sci. Eng., A*, 445–446 (2007) 113–121.
- [40] N. Sahai, Is silica really an anomalous oxide? Surface acidity and aqueous hydrolysis revisited, *Environ. Sci. Technol.*, 36 (2002) 445–452.
- [41] CRC, Handbook of Chemistry and Physics, 79th ed., CRC Press: Boca Raton, FL, 1998, pp. 12–15.
- [42] G.V. Buxton, C.L. Greenstock, W.P. Helman, A.B. Ross, Critical review of rate constants for reactions of hydrated electrons, hydrogen atoms and hydroxyl radicals in aqueous solution, *J. Phys. Chem. Ref. Data*, 17 (1988) 513–886.
- [43] H. Liu, Y. Yang, J. Kang, M. Fan, J. Qu, Removal of tetracycline from water by Fe–Mn binary oxide, *J. Environ. Sci.*, 24 (2012) 242–247.
- [44] P. Mahamallik, S. Saha, A. Pal, Tetracycline degradation in aquatic environment by highly porous MnO_2 nanosheet assembly, *Chem. Eng. J.*, 276 (2015) 155–165.
- [45] N. Li, X. Lu, S. Zhang, A novel reuse method for waste printed circuit boards as catalyst for wastewater bearing pyridine degradation, *Chem. Eng. J.*, 257 (2014) 253–261.
- [46] W.P. Kwan, B.M. Voelker, Rates of hydroxyl radical generation and organic compound oxidation in mineral-catalyzed Fenton-like systems, *Environ. Sci. Technol.*, 37 (2003) 1150–1158.
- [47] A.J. Bailey, W.P. Griffith, B.C. Parkin, Studies on polyoxo- and polyperoxometalates. Part 2. Heteropolyperoxo- and isopolyperoxo-tungstates and -molybdates as catalysts for the oxidation of tertiary amines, alkenes and alcohols, *J. Chem. Soc., Dalton Trans.*, 11 (1995) 1833–1837.
- [48] H.C. Shi, X.Y. Wang, R.M. Hua, Z.G. Zhang, J. Tang, Epoxidation of unsaturated acids catalyzed by tungstate (VI) or molybdate (VI) in aqueous solvents: a specific direct oxygen transfer mechanism, *Tetrahedron*, 61 (2005) 1297–1307.
- [49] J.M. Lin, M.L. Liu, Singlet oxygen generated from the decomposition of peroxymonocarbonate and its observation with chemiluminescence method, *Spectrochim. Acta A.*, 72 (2009) 126–132.
- [50] I. Dalmázio, M.O. Almeida, R. Augusti, Monitoring the degradation of tetracycline by ozone in aqueous medium via atmospheric pressure ionization mass spectrometry, *J. Am. Soc. Mass. Spectrom.*, 18 (2007) 679–687.
- [51] E. Yamal-Turbay, E. Jaén, M. Graells, M. Pérez-Moya, Enhanced photo-Fenton process for tetracycline degradation using efficient hydrogen peroxide dosage, *J. Photochem. Photobiol., A*, 267 (2013) 11–16.
- [52] B. Kakavandi, A. Takdastan, N. Jaafarzadeh, M. Azizi, A. Mirzaei, A. Azari, Application of $\text{Fe}_3\text{O}_4/\text{C}$ catalyzing heterogeneous UV-Fenton system for tetracycline removal with a focus on optimization by a response surface method, *J. Photochem. Photobiol., A*, 314 (2016) 178–188.

Supplementary material

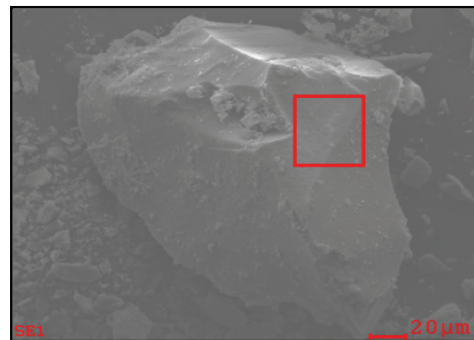
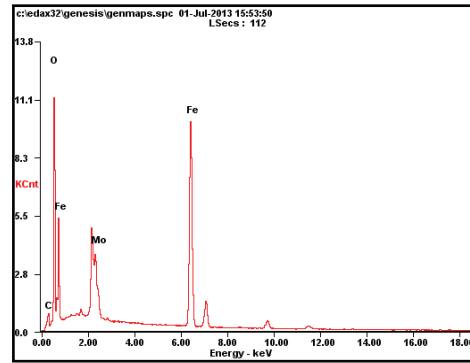
(1) Mo:Fe=0



<i>Element</i>	<i>Wt%</i>	<i>At%</i>
<i>CK</i>	02.03	06.30
<i>OK</i>	16.99	39.62
<i>FeK</i>	80.98	54.09
<i>Matrix</i>	Correction	ZAF

Fig. S1. Element composition for catalyst powder at Mo:Fe = 0.

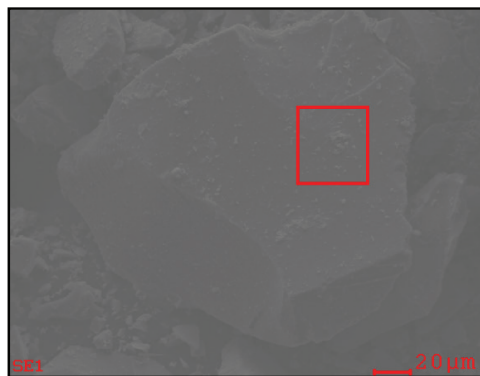
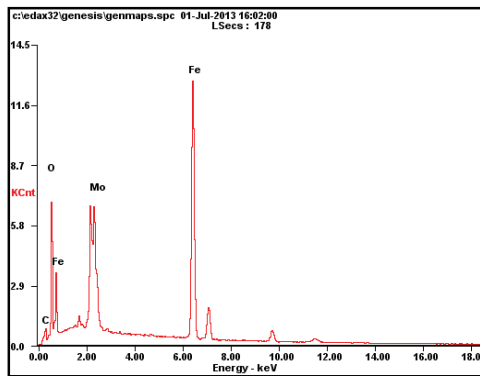
(2) Mo:Fe=0.1



<i>Element</i>	<i>Wt%</i>	<i>At%</i>
<i>CK</i>	03.33	09.74
<i>OK</i>	21.02	46.15
<i>MoL</i>	13.17	04.82
<i>FeK</i>	62.48	39.29
<i>Matrix</i>	Correction	ZAF

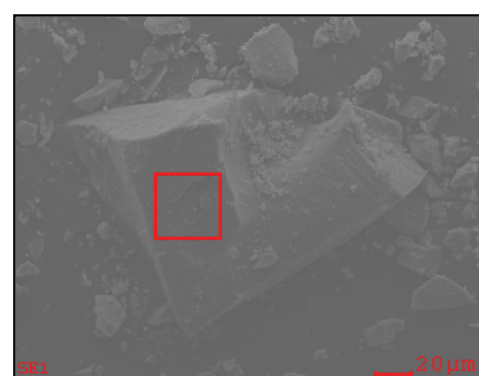
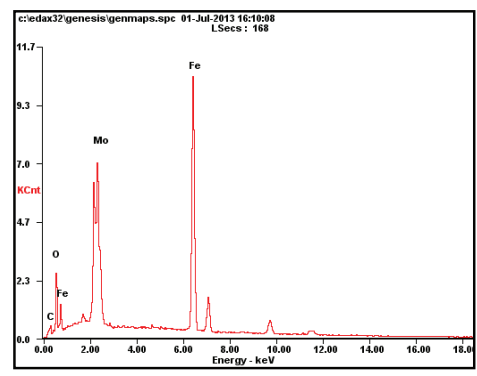
Fig. S2. Element composition for catalyst powder at Mo:Fe = 0.1.

(3)Mo:Fe=0.2



Element	Wt%	At%
CK	02.70	09.46
OK	12.57	33.09
MoL	20.48	08.99
FeK	64.25	48.46
Matrix	Correction	ZAF

(4)Mo:Fe=0.5

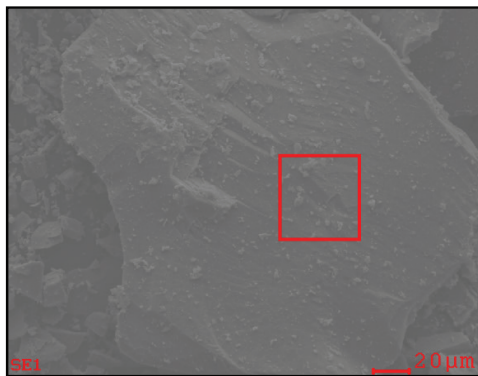
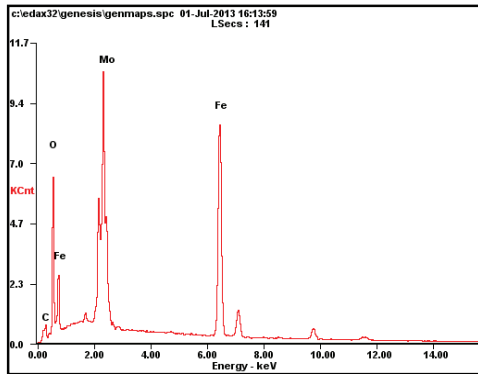


Element	Wt%	At%
CK	02.07	08.58
OK	06.50	20.21
MoL	27.28	14.13
FeK	64.14	57.08
Matrix	Correction	ZAF

Fig. S3. Element composition for catalyst powder at Mo:Fe = 0.2.

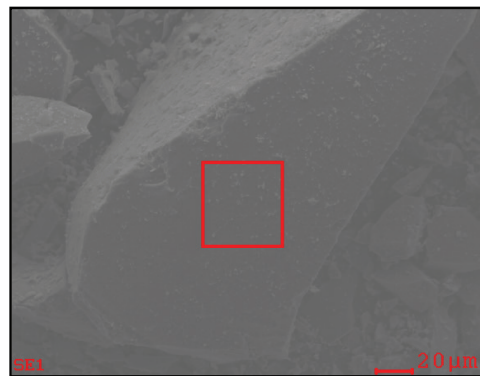
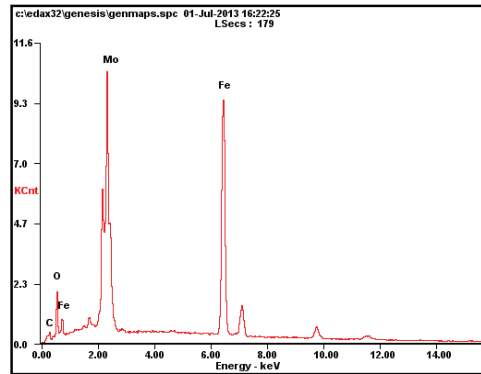
Fig. S4. Element composition for catalyst powder at Mo:Fe = 0.5.

(5) Mo:Fe=0.9



<i>Element</i>	<i>Wt%</i>	<i>At%</i>
<i>CK</i>	02.76	09.46
<i>OK</i>	15.66	40.34
<i>MoL</i>	32.44	13.94
<i>FeK</i>	49.14	36.26
<i>Matrix</i>	Correction	ZAF

(6) Mo:Fe=1.5



<i>Element</i>	<i>Wt%</i>	<i>At%</i>
<i>CK</i>	01.73	07.76
<i>OK</i>	04.98	16.75
<i>MoL</i>	35.86	20.12
<i>FeK</i>	57.43	55.37
<i>Matrix</i>	Correction	ZAF

Fig. S5. Element composition for catalyst powder at Mo:Fe = 0.9.

Fig. S6. Element composition for catalyst powder at Mo:Fe = 1.5.

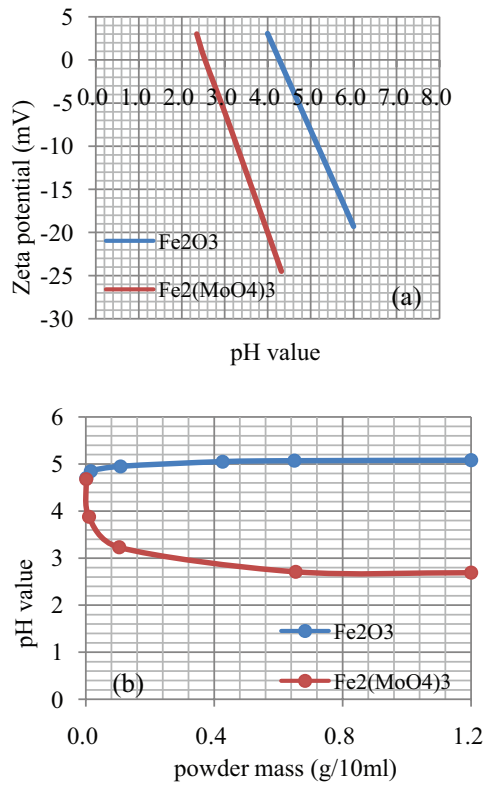


Fig. S7. PZC determination of Fe₂O₃ and Fe₂(MoO₄)₃.

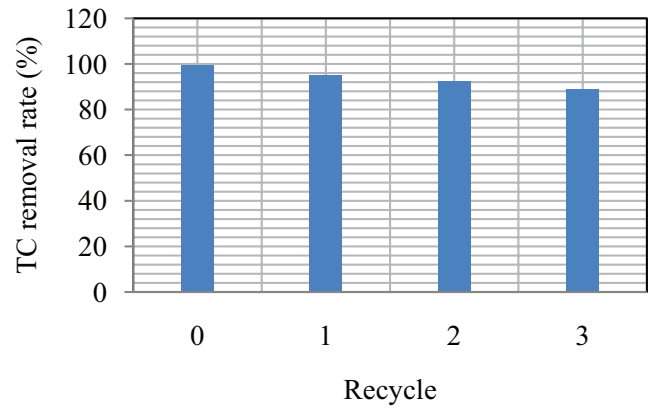


Fig. S8. Recycle use of Fe₂(MoO₄)₃.